



ELSEVIER

Journal of Chromatography A, 781 (1997) 3–10

JOURNAL OF
CHROMATOGRAPHY A

A simple means of generating pH gradients in capillary zone electrophoresis

Wayne E. Rae¹, Jennifer E. Wong, Charles A. Lucy*

Department of Chemistry, The University of Calgary, 2500 University Drive N.W., Calgary, Alberta, T2N 1N4, Canada

Abstract

Injection of a “pulse” of a secondary pH buffer just prior to the injection of analyte provides a mild pH gradient within the primary pH buffer. Separations of weakly acid or basic analytes are easily optimized using this gradient. A model explaining the impact of the pulse of secondary buffer is proposed. Experiments verify that the strength of the pH gradient depends on the effective width of the pulse, the difference in mobility of the analyte in the two buffers and on the difference in mobility between the analyte and the pulse of secondary buffer. Sixteen chlorinated phenols are baseline separated in 25 min using a 45-mM phosphate–15 mM tetraborate buffer (adjusted to pH 7.0) when 2.6% of the capillary is filled with 22.5 mM phosphate–7.5 mM tetraborate (adjusted to pH 10.0). © 1997 Elsevier Science B.V.

Keywords: pH gradients; Buffer composition; Phenols; Chlorophenols

1. Introduction

Over the past decade and a half, capillary zone electrophoresis (CZE) has demonstrated exceptional separating power. Separation efficiencies in excess of one million theoretical plates have been achieved [1]. Separations have been performed in as little as 1.5 s [2]. CZE has even separated isotopes [3]. However, for all of its strengths, CZE is essentially a one-dimensional technique — all analytes are separated under a single electrolyte condition. Many parameters, such as buffer pH [4,5] and the addition of surfactants and cyclodextrins, can alter the mobility of an analyte. However, it is not always possible to find an “optimum” condition that offers adequate separation for all components of interest, particularly

with complex samples, such as are found in environmental and biological systems.

In gas and liquid chromatography, this problem is commonly circumvented by the use of gradient techniques. Separations have been demonstrated in CZE using flow gradients [6] and in micellar electrokinetic chromatography (MEKC) using organic modifier gradients [7]. However, most previous work on gradient separations in capillary electrophoresis has dealt with pH gradients. Foret et al. [8] generated a step pH gradient by altering the pH within the inlet reservoir to optimize the CZE separation of proteins within a coated capillary. Tsuda [9] used a liquid chromatographic solvent gradient pump to control the mixing of two buffer solutions during the separation. Chang and Yeung [6] used a similar approach to generate dynamic pH gradients from pH 3.0 to 5.2 or flow gradients by the addition of a cationic surfactant. Alternatively, binary gradients have been generated using electroosmotic flow pumping [10,11]. However, all of these techniques require

*Corresponding author.

¹Current address: Enviro-Test Laboratories, Bay #2, 1313-44th Avenue NE, Calgary, Alberta, Canada

custom equipment and, so, cannot be utilized with commercial instrumentation.

Whang and Yeung [12] introduced an ingenious procedure for performing pH gradients. Using an electrolyte buffer with a large temperature coefficient (dpH/dT), such as Tris, a pH step or gradient is generated by altering the temperature of the buffer. This temperature change is achieved either using the external circulating coolant surrounding the capillary [12] or by exploiting Joule heating within the capillary [13]. However, this approach is limited to buffers that possess a large temperature coefficient.

In this work, we discuss and characterize dynamic pH gradients generated by injection of a short segment of a second buffer. This approach is similar to the “dynamic pulse” technique first discussed by Boček et al. [14] and to electrophoretically mediated microanalysis (EMMA) techniques [15–19]. The generation of dynamic pH gradients in this manner is probed using a series of model solutes possessing similar acid dissociation constants. The technique is then applied to the separation of sixteen chlorinated phenols.

2. Experimental

2.1. Apparatus

All experiments were performed on a Beckman P/ACE 2100 CE system (Fullerton, CA, USA), equipped with on-column UV absorbance detection. The electrodes were in the normal configuration (i.e., sample was loaded at the anode and the detector was positioned 7 cm from the cathode). Fused-silica capillaries were from Polymicro Technologies (Phoenix, AZ, USA) and had an internal diameter of 75 μm and an outer diameter of 375 μm . The capillary length was 77 cm long (70 cm to detector) for studies using chlorophenols and 47 cm (40 cm to detector) for other studies. System Gold software (Beckman, version 7.11), operating on a 386-based microcomputer, was used for data acquisition (5 Hz) and control.

2.2. Reagents

All reagent solutions were prepared using distilled

deionized water (Nanopure Water System, Barnstead, Dubuque, IA, USA). Analytical grade reagents were used throughout.

Stock solutions of each chlorinated phenol were prepared using the pure components, obtained from Aldrich (Milwaukee, WI, USA). The minimum purity of each component was 95%. Each of the sixteen chlorinated phenols was individually weighed into separate 100 ml volumetric flasks, and brought to volume with ACS reagent grade methanol (BDH, Toronto, Canada). These stock solutions were used to spike desired levels of the chlorinated phenols into buffer solutions. The methanol concentration in each of the standard solutions was maintained constant at 1.2%.

2.3. Procedures

Prior to use, new capillaries were pretreated by a 10-min rinse with 0.1 *M* sodium hydroxide (BDH). All experiments were conducted at 25°C. The detection wavelength was 214 nm. Before each run, the capillary was rinsed for 1 min with 0.1 *M* sodium hydroxide and then for 1 min with the electrophoretic buffer. Sample was injected hydrodynamically by applying 3.5 kPa (0.5 p.s.i.) of pressure to the sample vial for 10 s. Other experimental conditions specific to a given study are listed below.

3. Results and discussion

Fig. 1 illustrates the procedure used to generate dynamic pH gradients. In Fig. 1A, the capillary is filled with an initial buffer. A small “pulse” or segment of a second buffer is then introduced onto the capillary (Fig. 1B), followed by the sample (Fig. 1C). Upon application of the voltage (Fig. 1D), the sample analytes and the “pulse” all migrate. However, the migration rates of each may differ.

The effect of this differential migration and associated acid/base effects is demonstrated schematically in Fig. 2. In this figure, the *x*-axis represents the physical position along the capillary and the *y*-axis represents the time. The lines and shaded band represent the migration of three solutes and the pulse of the second buffer, respectively. For simplicity,

A) Rinse capillary with primary buffer



B) Inject pulse of secondary buffer at inlet.



C) Inject sample at inlet.



D) Apply voltage to perform electrophoretic separation.



Fig. 1. Schematic representation of the procedure used to generate a pH gradient using a dynamic pulse: (A) Capillary rinsed with primary buffer (1°); (B) secondary buffer (2°) injected hydrodynamically; (C) analytes (black line) injected hydrodynamically and (D) electrophoretic separation assuming no broadening or inter-mixing of the buffer zones.

Figs. 1D and 2 assume that the pulse of secondary buffer undergoes no broadening or mixing with the primary buffer. The slope of each of the lines indicates the local migration velocity. Line A represents a solute whose apparent mobility is slower than the "pulse" of buffer. The slow solute and the pulse of secondary buffer do not intersect. As a result, solute A elutes at the migration time characteristic of its migration in the initial buffer. Solute B and C possess apparent mobilities that are slightly faster than the pulse of the second buffer. Upon overlapping with the shaded area in Fig. 2, these solutes experience a different pH. If the new pH alters the ionization of the solute such that it has a more rapid apparent mobility (solute B), the solute will elute earlier than for migration in the initial buffer alone.

Alternatively, if the solute has a slower apparent mobility in the secondary buffer zone (solute C), the migration time for the solute increases. Thus, despite solutes B and C being poorly resolved in the initial buffer (lines are nearly parallel), their different responses to the pulse of secondary buffer yields clear separation.

Simplifying assumptions of no band broadening, no mixing between the primary and secondary buffer systems and of an infinitely narrow sample injection plug are used to derive the following model. Under these idealized conditions, the interaction time between a solute and the pulse of secondary buffer ($t_{\text{interaction}}$) is given by [15]:

$$t_{\text{interaction}} = w/(v_2 - v_p) \quad (1)$$

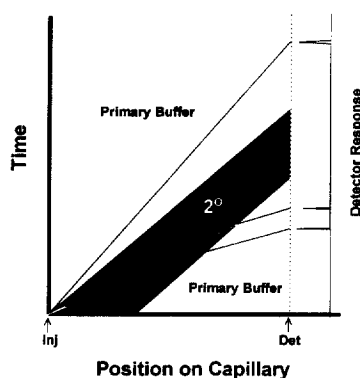


Fig. 2. Electrophoretic movement of analytes in the presence of a dynamic pulse of secondary buffer. Analytes A, B and C migrate through the capillary from the capillary inlet (INJ) to the detector (DET) near the outlet. The dynamic pulse (shaded) of secondary buffer is assumed not to broaden or mix with the primary buffer. In the primary buffer, A has the lowest effective mobility, while B and C possess similar mobilities. B and C have different mobilities in the secondary buffer and are separated due to their interaction with the dynamic pulse. Adapted from Fig. 1 of reference [14].

where w is the width of the pulse of secondary buffer; v_2 is the velocity of the analyte in the secondary buffer and v_p is the velocity of the pulse of secondary buffer. The observed analyte velocity (v_{obs}) is the sum of the analyte velocity in each

buffer times the fraction of the capillary length (L_d) that the analyte traveled in that buffer:

$$v_{obs} = [(t_{interaction} v_2)/L_d]v_2 + [(L_d - t_{interaction} v_2)/L_d]v_1 \quad (2)$$

Substituting Eq. (1) into Eq. (2) and rearranging yields:

$$v_{obs} = v_1 + (w/L_d)v_2(v_2 - v_1)/(v_2 - v_p) \quad (3)$$

This expression indicates the effect of a number of experimental parameters involved with the dynamic pulse gradient on the observed migration rates. The following sections detail investigations of these parameters.

3.1. Effect of width of pulse of secondary buffer

Eq. (3) indicates that the effect of the width of the pulse of secondary buffer (w) should be directly related to the change in the velocity of the solute. To test this behavior, five model solutes were used. These solutes possess similar acid dissociation constants, but different mobilities. These solutes are listed in Table 1 in order of their mobility, from fastest cation to fastest anion. In Table 1a, the mobility of each of these solutes is altered by the pH

Table 1
Effect of width of dynamic pulse on analyte migration

Pulse width (s)	(a) Analyte electrophoretic mobility ($\text{cm}^2/\text{Vs}) \times 10^4$				
	Imidazole	Papaverine	2,4,5-Trichlorophenol	2,6-Dichlorophenol	2-Nitrophenol
0	3.25	0.84	-0.45	-0.57	-0.83
20	2.53	0.72	-1.47	-1.97	-2.10
30	2.23	0.64	-1.83	-2.40	-2.62
40	1.82	0.46	-2.21	-2.77	-2.89
50	1.49	0.37	-2.49	-2.88	-2.98
	(b) Apparent pH causing analyte migration				
0	6.00	6.00	6.00	6.00	6.00
20	6.43	6.15	6.97	7.23	7.06
30	6.59	6.26	7.25	7.63	7.58
40	6.85	6.47	7.56	8	8.7
50	7.05	6.66	8.13	>9	>9

^aExperimental conditions: isocratic, 45 mM phosphate–15 mM tetraborate buffer (adjusted to pH 6.0); gradient, isocratic plus a (3.5 kPa) dynamic pulse of 30 mM phosphate–10 mM tetraborate buffer (adjusted to pH 10.0); voltage, 10.0 kV; temperature, 25°C; detection, 214 nm; injection, 10 s hydrodynamic (3.5 kPa).

gradient generated by the pulse of secondary buffer. As would be expected, the pulse of pH 10.0 buffer lowers the electrophoretic mobilities of the amines and increases the electrophoretic mobility of the phenols. The change in mobility with pulse width is monotonic, but not linear. Thus, qualitatively, Eq. (3) is obeyed.

The non-linearity in the mobility change noted above suggests that the primary and secondary buffer zone do interact, contrary to the assumption made in deriving Eq. (3). If the primary and secondary buffers do interact, and neutralize one another, there will be a zone of intermediate pH in the vicinity of the analyte injection. The precise pH and width of this zone will be a complex relationship between the relative buffering capacities of the two buffers and the injected width of the pulse of secondary buffer. Further evidence that the two buffers do interact is given in Table 2. If the assumption that the buffers do not interact were true, the concentration of the secondary buffer should have no effect on the observed mobilities. However, as can be seen in Table 2a, the concentration of the secondary buffer has a distinct impact on the mobility of all of the analytes. If a higher concentration of secondary

buffer (phosphate–tetraborate buffer, pH 10) is used, then the analyte behaves as if it were migrating in a more alkaline buffer.

To better illustrate the effect of the pulse of secondary buffer on the analyte's mobility, the following approach was used. Plots (not shown) were generated of the electrophoretic mobility of each of the analytes versus the pH of the primary buffer (45 mM phosphate–15 mM borate) from pH 5.5. to 9.0. These plots demonstrated the expected sigmoidal shape [4]. The analyte's mobility observed within the gradient experiments was then related to an "apparent pH" from this isocratic data. This approach is analogous to the apparent column temperature commonly used in temperature gradient gas chromatography. The mobility data in Tables 1a and 2a is presented again in terms of apparent pH in Tables 1b and 2b. As can be seen in these tables, increasing either the pulse width or the secondary buffer concentration increases the change in the apparent pH at which the analyte migrates. Not surprisingly, it was also found that the strength of the pH gradient could be controlled by altering the pH of the secondary buffer.

One caveat should be raised. Use of a gradient that

Table 2
Effect of concentration of secondary buffer on analyte migration^a

Pulse buffer ^b (Conc, mM)	(a) Analyte electrophoretic mobility (cm ² /Vs) × 10 ⁴				
	Imidazole	Papaverine	2,4,5-Trichlorophenol	2,6-Dichlorophenol	2-Nitrophenol
15/5	2.88	0.90	−1.06	−1.44	na
30/10	2.53	0.73	−1.47	−1.97	−2.10
45/15	2.14	0.53	−1.75	−2.31	−2.53
60/20	1.70	0.36	−2.00	−2.57	−2.81
75/25	1.33	0.28	−2.22	−2.79	−2.93
90/30	0.97	0.24	−2.40	−2.84	−2.96
	(b) Apparent pH causing analyte migration				
15/5	6.20	5.92	6.62	6.73	na
30/10	6.43	6.15	6.97	7.23	7.06
45/15	6.66	6.4	7.19	7.54	8.19
60/20	6.93	6.68	7.37	7.81	8.07
75/25	7.16	6.85	7.57	8.11	>9
90/30	7.37	6.99	7.87	8.40	>9

^aExperimental conditions: isocratic, 45 mM phosphate–15 mM tetraborate buffer (adjusted to pH 6.0); gradient, isocratic plus 20 s (3.5 kPa) dynamic pulse of phosphate–tetraborate buffer (adjusted to pH 10.0); voltage, 10.0 kV; temperature, 25°C; detection, 214 nm; injection, 10 s hydrodynamic (3.5 kPa).

^bBuffer concentration is given in "millimolar phosphate"/"millimolar tetraborate".

is too strong, formed either by the use of a long pulse or by a concentrated secondary buffer, results in additional peak broadening.

3.2. Effect of the difference in analyte mobility between the two buffers

For a monoprotic weakly acidic analyte, the observed solute mobility (μ_{obs}) is given by [4]:

$$\mu_{\text{obs}} = K_a / ([\text{H}^+] + K_a) \mu_{\text{A}^-} \quad (4)$$

where: μ_{A^-} is the mobility of the fully ionized form of the acid and K_a is the acid dissociation constant for the analyte. Thus, the greatest change in mobility occurs when the buffer pH is close to the acid dissociation constant of the analyte. Since the effect of the pulse of secondary buffer is directly related to the difference in the mobility of the analyte between the two buffers (Eq. (3)), the effect of the pulse of secondary buffer should be greatest when the pH of the primary buffer is close to the acid dissociation constant of the analyte.

The effect of pH on the effectiveness of the pulse of secondary buffer was investigated using fifteen chlorinated phenols as the model solutes [20]. The acid dissociation constants of these solutes vary from 4.74 for pentachlorophenol to 9.37 for 4-chlorophenol [21]. The mobility of these analytes was first determined under isocratic pH 7.0 conditions and then using a pulse of pH 10 buffer. Fig. 3 is a plot of the mobility difference observed upon injection of a pulse of buffer, pH 10, versus the acid dissociation constants of the chlorinated phenols. The effect of the dynamic pulse is greatest when the acid dissociation constant of the analyte is close to the pH of the primary electrolyte (pH 7.0 in Fig. 3), as expected from Eq. (4). Also, as expected, the effect of the dynamic pulse diminishes as the acid dissociation constant becomes significantly greater than the primary buffer pH of 7.0. Ideally, the same behavior is expected for analytes with acid dissociation constants that are less than the buffer pH. However, in this case, the observed behavior is confounded by these same analytes (multi-chlorinated phenols) also possessing the highest mobilities at pH 7.0. In Section 3.3, high mobilities for anions are shown to magnify

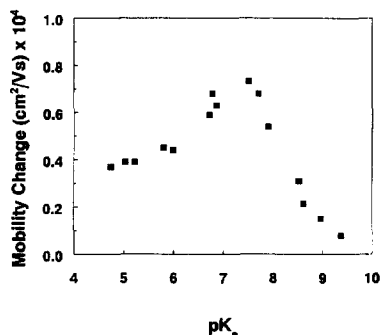


Fig. 3. Change in mobility of fifteen chlorinated phenols between isocratic buffer conditions, pH 7.0, and a pH gradient generated by a dynamic pulse of buffer at pH 10. Experimental conditions: isocratic buffer, 45 mM phosphate–15 mM tetraborate, adjusted to pH 7.0; gradient, as in isocratic but with an 8% capillary length dynamic pulse of 22.5 mM phosphate–7.5 mM tetraborate, adjusted to pH 10; voltage, 22 kV; capillary, 77 cm × 75 μm ; temperature, 25°C; injection, 10 s hydrodynamic (3.5 kPa) and detection, 214 nm.

the effects of a pulse of phosphate–tetraborate buffer, pH 10.

3.3. Effect of the mobility of the analyte relative to the mobility of the buffer pulse

Eq. (3) predicts that the effect of the pulse of secondary buffer should be greatest if the mobility of the solute is similar to that of the pulse. Given that the pulse of secondary buffer interacts with the primary buffer (Section 3.1), it is impossible to predict the mobility of the pulse. Nevertheless, some relation would be expected between analyte mobility and the impact of the pulse. To test this hypothesis, five model solutes possessing similar acid dissociation constants, but with different mobilities were used. These solutes are listed in Table 3 in order of their mobility, from the fastest cation to the fastest anion. Column 3 of the table is an estimate of the mobility of the fully ionized form of the solute. Column 4 is the electrophoretic mobility of the solute within the primary buffer (phosphate–tetraborate buffer, pH 6.0). Column 5 shows the mobility observed when a 20-s (3.5 kPa) pulse of phosphate–tetraborate buffer, pH 10.0, was injected just before the sample. All of the solutes, regardless of their mobility, display significant effects due to the dynamic pulse. However, the relative magnitude of the

Table 3
Effect of mobility of the analyte on the effect of buffer pulse^a

Solute	p <i>K</i> _a	Mobility (cm ² /Vs) × 10 ⁴			Apparent ph
		Fully ionized	Isocratic	Gradient	
Imidazole	6.95	3.8 ^b	3.25	2.14	6.66
Papaverine	6.40	1.2 ^b	0.84	0.53	6.4
2,4,5-Trichlorophenol	6.72	-2.5 ^c	-0.45	-1.15	7.19
2,6-Dichlorophenol	6.78	-2.8 ^c	-0.57	-2.31	7.54
2-Nitrophenol	7.17	-2.9 ^c	-0.83	-2.53	8.19

^aExperimental conditions: isocratic, 45 mM phosphate–15 mM tetraborate buffer (adjusted to pH 6.0); gradient, isocratic plus 20 s (3.5 kPa) dynamic pulse of 45 mM phosphate–15 mM tetraborate buffer (adjusted to pH 10.0); voltage, 10.0 kV; temperature, 25°C; detection, 214 nm; injection, 10 s hydrodynamic (3.5 kPa).

^bEstimated as the mobility in 45 mM phosphate–15 mM tetraborate buffer (pH 5.5). All other conditions as in ^a.

^cEstimated as the mobility in 45 mM phosphate–15 mM tetraborate buffer (pH 9.0). All other conditions as in ^a.

effect appears to increase as one goes down Column 5 [i.e., from imidazole (fastest cation) to 2-nitrophenol (fastest anion)]. This trend is more clearly presented by the “apparent pH” under which the analytes move under these gradient conditions. In general, the apparent pH becomes more alkaline as the analyte’s mobility moves from fastest cationic to fastest anionic. That is, the faster the analyte migrates towards the anode, the greater the effect of the pulse of phosphate–tetraborate pulse, pH 10. It is noteworthy that the buffer ions (phosphate and tetraborate) would both migrate towards the anode as well, and may possibly then influence the migration of the pulse within the capillary. Such an anodic migration is consistent with the trend noted in Table 3. However, at this time it is not possible to make any definitive predictions regarding the movement of the pulse of secondary buffer.

To summarize, the mobility of the analyte has an impact on the effectiveness of the dynamic pulse, as was predicted by Eq. (3).

3.4. Application

In a previous study, the separation of sixteen chlorinated phenols was optimized under isocratic pH conditions [22]. It was found that the early eluting monochlorinated phenols were best separated at pH values greater than eight, while the later-eluting multi-chlorinated phenols were best separated at pH 7. An optimum separation was achieved using 45 mM phosphate–0.15 mM tetraborate buffer at a compromise pH of 7.3. Under these conditions, the

critical separations were: *p*- and *m*-chlorophenol with a resolution of 0.4; and 3,4-di- and *o*-chlorophenol with a resolution of 0.6. This same separation was optimized using 45 mM phosphate–0.15 mM tetraborate buffer adjusted to pH 7.0 as the primary buffer and 22.5 mM phosphate–7.5 mM tetraborate adjusted to pH 10.0 as the secondary buffer. Pulse lengths of 0.13 to 8% of the capillary length were investigated [20]. In all cases, the resolution of the critical pairs was improved, achieving resolutions of 1.6 and 1.5, respectively, for the 8% pulse. Fig. 4 shows the separation of the sixteen chlorinated phenols using the pulse method to generate pH gradient conditions. This separation is clearly superior to those achieved previously using isocratic pH conditions [22,23].

4. Conclusions

Use of a pulse of secondary buffer is an easy and convenient means of generating mild pH gradients in capillary zone electrophoresis. The impact of the pulse on analyte migration is a function of: the strength of the pulse, as determined by the pulse width; the pH and the buffering capacity; the difference in mobility of the analyte between the two pH conditions, which is influenced by the relationship between the primary buffer pH and the analyte acid dissociation constant; and by the difference in mobility between the analyte and the pulse. Excessively strong pulses can lead to undesirable band broadening and should be avoided.

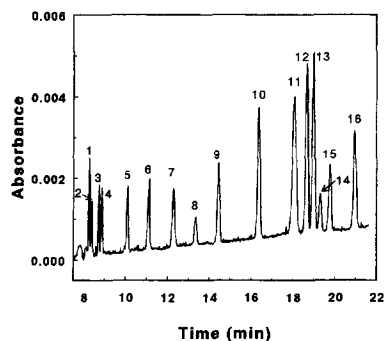


Fig. 4. Separation of sixteen chlorinated phenols using a pH gradient generated with a dynamic pulse. Peaks: 1=*p*-chlorophenol; 2=*m*-chlorophenol; 3=3,4-dichlorophenol; 4=*o*-chlorophenol; 5=2,4-dichlorophenol; 6=2,3-dichlorophenol; 7=2,5-dichlorophenol; 8=2,3,4-trichlorophenol; 9=2,4,5-trichlorophenol; 10=2,3,5-trichlorophenol; 11=2,6-dichlorophenol; 12=2,4,6-trichlorophenol; 13=pentachlorophenol; 14=2,3,4,6-tetrachlorophenol; 15=2,3,5,6-tetrachlorophenol and 16=2,3,6-trichlorophenol. Experimental conditions: primary buffer, 45 mM phosphate–15 mM tetraborate, adjusted to pH 7.0; pulse, 2.6% of capillary with 22.5 mM phosphate–7.5 mM tetraborate, adjusted to pH 10; voltage, 22 kV; capillary, 77 cm × 75 μm; temperature, 25°C; injection, 10 s hydrodynamic (3.5 kPa) and detection, 214 nm.

Acknowledgments

Financial support from the Natural Sciences and Engineering Research Council of Canada and The University of Calgary are gratefully acknowledged. Funding provided for J.E.W. by the Summer Career Placements Program of the Government of Canada is gratefully acknowledged. W.E.R. would also like to thank the Alberta Heritage Scholarship Fund for support in the form of the Wilfred R. May Scholarship for Career Development.

References

- [1] J.W. Jorgenson, K.D. Lukacs, *Science* 222 (1983) 266–272.
- [2] C.A. Monning, J.W. Jorgenson, *Anal. Chem.* 63 (1991) 802–807.
- [3] C.A. Lucy, T.L. McDonald, *Anal. Chem.* 67 (1995) 1074–1078.
- [4] S.C. Smith, M.G. Khaledi, *Anal. Chem.* 65 (1993) 193–198.
- [5] J.L. Beckers, F.M. Everaerts, M.T. Ackermans, *J. Chromatogr.* 537 (1991) 407–428.
- [6] H.-T. Chang, E.S. Yeung, *J. Chromatogr.* 608 (1992) 65–72.
- [7] A.T. Balchunas, M.J. Sepaniak, *Anal. Chem.* 60 (1988) 617–621.
- [8] F. Foret, S. Fanali, P. Boček, *J. Chromatogr.* 516 (1990) 219–222.
- [9] T. Tsuda, *Anal. Chem.* 64 (1992) 386–390.
- [10] P. Boček, M. Deml, J. Pospíchal, J. Sudor, *J. Chromatogr.* 470 (1989) 309–312.
- [11] V. Purgart, D.E. Games, *J. Chromatogr.* 605 (1992) 139–142.
- [12] C.-W. Whang, E.S. Yeung, *Anal. Chem.* 64 (1992) 502–506.
- [13] H.-T. Chang, E.S. Yeung, *J. Chromatogr.* 632 (1993) 149–155.
- [14] P. Boček, M. Deml, J. Pospíchal, *J. Chromatogr.* 500 (1990) 673–680.
- [15] B.J. Harmon, D.H. Patterson, F.E. Regnier, *Anal. Chem.* 65 (1993) 2655–2662.
- [16] B.J. Harmon, I. Leesong, F.E. Regnier, *Anal. Chem.* 66 (1994) 3797–3805.
- [17] D.H. Patterson, B.J. Harmon, F.E. Regnier, *J. Chromatogr. A* 662 (1994) 389–395.
- [18] B.J. Harmon, F.E. Regnier, D.H. Patterson, *Trends Anal. Chem.* 14 (1995) 177.
- [19] S. Liu, P.K. Dasgupta, *Anal. Chim. Acta* 268 (1992) 1–6.
- [20] W.E. Rae, M.Sc. thesis, University of Calgary, September 1996.
- [21] R.C. Weast (Editor), *Handbook of Chemistry and Physics*, CRC Press, Boca Raton, FL, 60th ed., 1980.
- [22] W.E. Rae and C.A. Lucy, *J. Assoc. Off. Anal. Chem. Int.*, submitted Dec. 1996.
- [23] M.F. Gonnord, J. Collet, *J. Chromatogr.* 645 (1993) 327–336.